

Supplemental Material for: “Electro-optic tuning of single-frequency ultra-narrow linewidth microdisk laser”

Jintian Lin,^{a,g,#} Saeed Farajollahi,^{b,#} Zhiwei Fang,^{c,#} Ni Yao,^{d,e} Renhong Gao,^{a,g} Jianglin Guan,^{c,f} Li Deng,^{c,f} Tao Lu,^{b,*}, Min Wang,^{c,f} Haisu Zhang,^{c,f} Wei Fang,^{e,h,*} Lingling Qiao,^{a,g} and Ya Cheng^{a,c,f,g,i,j,k,*}

^aState Key Laboratory of High Field Laser Physics and CAS Center for Excellence in Ultra-Intense Laser Science, Shanghai Institute of Optics and Fine Mechanics (SIOM), Chinese Academy of Sciences (CAS), Shanghai, China, 201800

^bDepartment of Electrical and Computer Engineering, University of Victoria, Victoria, British Columbia, Canada, V8P 5C2

^cXXL—The Extreme Optoelectromechanics Laboratory, School of Physics and Electronic Science, East China Normal University, Shanghai, China, 200241

^dResearch Center for Intelligent Sensing, Zhejiang Lab, Hangzhou, China, 311100

^eThe Interdisciplinary Center for Quantum Information, State Key Laboratory of Modern Optical Instrumentation, College of Optical Science and Engineering, Zhejiang University, Hangzhou, China, 310027

^fState Key Laboratory of Precision Spectroscopy, East China Normal University, Shanghai, China, 200062

^gCenter of Materials Science and Optoelectronics Engineering, University of Chinese Academy of Sciences, Beijing, China, 100049

^hIntelligent Optics & Photonics Research Center, Jiaxing Institute of Zhejiang University, Jiaxing, China, 314031

ⁱCollaborative Innovation Center of Extreme Optics, Shanxi University, Taiyuan, China, 030006

^jCollaborative Innovation Center of Light Manipulations and Applications, Shandong Normal University, Jinan, China, 250358

^kShanghai Research Center for Quantum Sciences, Shanghai, China, 201315

[#]These authors contributed equally to the work.

*Address all correspondence to Tao Lu, taolu@ece.uvic.ca; Wei Fang, wfang08@zju.edu.cn; Ya Cheng, ya.cheng@siom.ac.cn.

1. The pump power dependent microlaser frequency tuning on MHz range

The tuning of the microlaser as a function of the pump power on MHz range can be resolved from the beat note signal from two identical single-mode microlasers that is captured by the RSA, as shown in Fig. S1(a). Here, one of the microlaser was pumped by a power stabilized laser, while the other microlaser was pumped by another laser whose power was carefully adjusted with a step of 1 μ W. The tuning efficiency was measured to be 1.54 MHz/ μ W with the linear fitting, which agrees well with the result measured by the OSA.

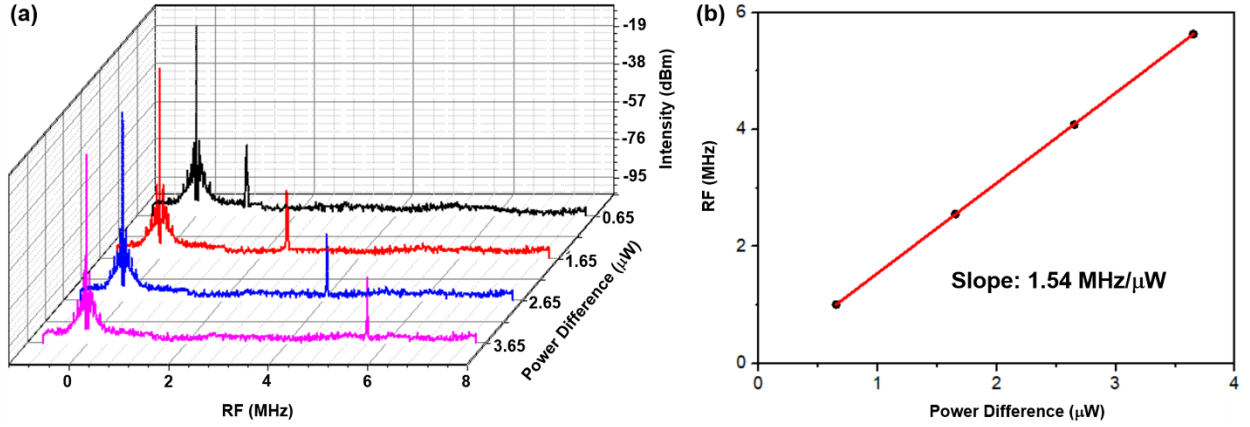


Fig. S1 (a) The RF spectra as functions of the pump power difference. (b) Power difference-dependent RF, showing a linear slope of 1.54 MHz/ μ W.

2. The design of the electrodes

Since the optical modes are TE polarized, the electric field interacts with the optical mode through the linear EO coefficient r_{22} ($= 6.8 \times 10^{-12}$ m/V). When the bias was applied to the electrodes, we choose new principal axes (x' , y' , z'), to eliminate the mixed terms in the equation of the ellipsoid, where z' is parallel to z , and x' and y' are rotated 45° with regard to x and y , as shown in Fig. S2.

The refractive indices in the x' and y' directions are

$$n_{x'} = n_o + \frac{1}{2}r_{22}(E_x + E_y)n_o^3, \quad (\text{S1a})$$

$$n_{y'} = n_o - \frac{1}{2}r_{22}(E_x + E_y)n_o^3, \quad (\text{S2b})$$

where, E_x and E_y are the electric field components established between the electrodes when an external bias voltage is applied, n_o is the ordinary index. If the electric field produced by the applied bias was axisymmetric, the average of effective index variation of TE polarized WGMs in one round induced by the bias is zero, which causes the zero shift of resonant wavelength. To achieve an effective index variation for the TE polarized wave, the outer plane electrode was designed with an opening of toward the $-y'$ direction ($\theta=3\pi/2$), as shown Fig. S2. In this case, the TE polarized

wave experiences an average refractive index increment of -0.0004 when the applied voltage was 300 V , leading to a predicted red-shifted resonant wavelength of $\sim 240\text{ pm}$ and a tuning efficiency of 80 pm/V , which is in good agreement with the measured result of 50 pm/V . The deviation between these two values maybe attributed to the heterogeneity of electric field along the microdisk circumference. To further improve the tuning efficiency, the outer plane electrode should be closer to the inner microelectrode.

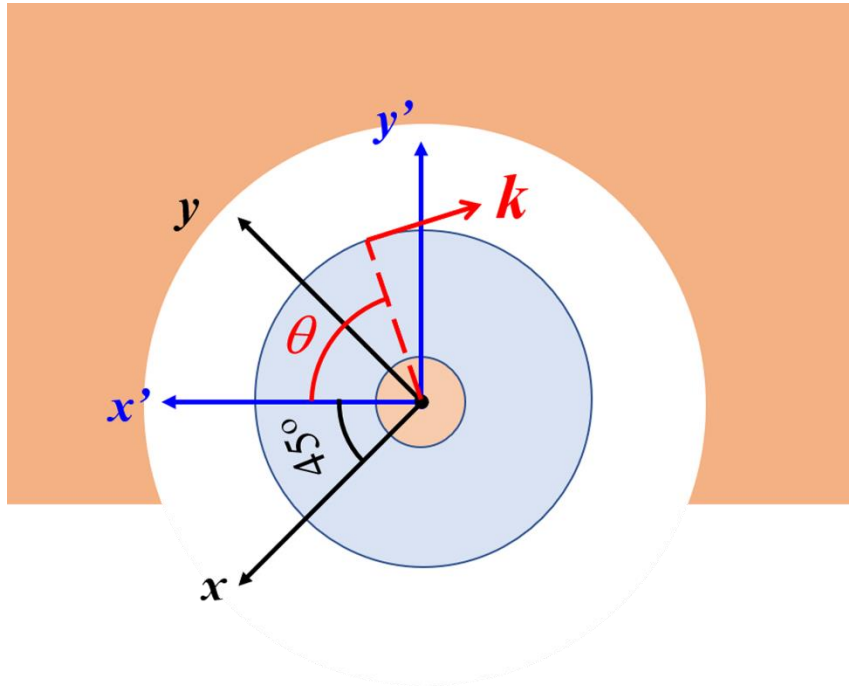


Fig. S2 The illustrated layout of the EO tuning of the microdisk, where k is wave vector.

3. The relationship between the pump threshold and the overlap integral

Here we illustrate the relation between overlap Γ vs pump threshold in the case where both laser and pump are in whispering gallery modes. Similar derivations could reach the same conclusion in the case where both modes are polygons of the same shape.

Assuming the scalar optical fields of pump $\Psi_p(\phi, \rho, z)$ and laser $\Psi_L(\phi, \rho, z)$ can be expressed in cylindrical coordinate (ϕ, ρ, z) as

$$\Psi_p(\phi, \rho, z) = a_p(\phi)e^{jm_p\phi}\Phi_p(\rho, z), \quad (\text{S3a})$$

$$\Psi_L(\phi, \rho, z) = a_L(\phi)e^{jm_L\phi}\Phi_L(\rho, z). \quad (\text{S3b})$$

Here, $m_p = m_{r,p} + jm_{i,p}$ is a complex number whose real part $m_{r,p}$ represents the azimuthal mode order of the pump mode and $m_{i,p}$ characterizes the cold cavity loss. Respectively, $m_L = m_{r,L} + jm_{i,L}$, and $m_{r,L}$ is the azimuthal mode order of the laser field. $\Phi_p(\rho, z)$ and $\Phi_L(\rho, z)$ are the whispering gallery modes of the pump wave and laser signal, both are normalized such that $|a_p(\phi)|^2$ and $|a_L(\phi)|^2$ are the powers of pump and laser at azimuthal angle ϕ . Accordingly, the intensities of pump I_p and laser I_L can be expressed as $I_p(\phi, \rho, z) = |a_p(\phi)|^2 \hat{I}_p(\rho, z)$ and $I_L(\phi, \rho, z) = |a_L(\phi)|^2 \hat{I}_L(\rho, z)$, $\hat{I}_p(\rho, z) = \Phi_p^*(\rho, z)\Phi_p(\rho, z)$, $\hat{I}_L(\rho, z) = \Phi_L^*(\rho, z)\Phi_L(\rho, z)$.

Also, in a three-level lasing system, one can write the rate equations as

$$\frac{dN_2(\phi, \rho, z)}{dt} = \frac{I_p(\phi, \rho, z)}{h\nu_p} N_1(\phi, \rho, z)\sigma_{13} + \frac{I_L(\phi, \rho, z)}{h\nu_L} N_1(\phi, \rho, z)\sigma_{12} - \frac{N_2(\phi, \rho, z)}{\tau_{sp}}, \quad (\text{S4a})$$

$$\frac{dI_p(\phi, \rho, z)}{\rho d\phi} = -N_1(\phi, \rho, z)\sigma_{13}I_p(\phi, \rho, z) - \frac{2m_{i,p}}{\rho}I_p(\phi, \rho, z), \quad (\text{S4b})$$

$$\frac{dI_L(\phi, \rho, z)}{\rho d\phi} = [N_2(\phi, \rho, z)\sigma_{21} - N_1(\phi, \rho, z)\sigma_{12}]I_L(\phi, \rho, z) - \frac{2m_{i,L}}{\rho}I_L(\phi, \rho, z), \quad (\text{S4c})$$

where h is the Planck's constant, ν_p and ν_L are pump and laser photon frequencies, τ_{sp} is the spontaneous emission lifetime, σ_{ij} is the decay rate per atom from energy level i to j , $N_1(\phi, \rho, z)$ and $N_2(\phi, \rho, z)$ are carrier densities at the 1st and 2nd energy levels at spatial location (ϕ, ρ, z) . Here we assume the rapid transition $3 \rightarrow 2$ such that all carriers pump to the 3rd level will quickly migrate to the 2nd level. Under such approximation, the total carrier density $N_T = N_1 + N_2$. Note at the steady state, $\frac{dN_2(\phi, \rho, z)}{dt} = 0$, we have

$$N_1(\phi, \rho, z) = \frac{1}{\left[\frac{I_p(\phi, \rho, z)}{h\nu_p} \sigma_{13} + \frac{I_L(\phi, \rho, z)}{h\nu_L} \sigma_{12} \right] \tau_{sp} + 1} N_T, \quad (\text{S5a})$$

$$N_2(\phi, \rho, z) = \frac{\left[\frac{I_p(\phi, \rho, z)}{h\nu_p} \sigma_{13} + \frac{I_L(\phi, \rho, z)}{h\nu_L} \sigma_{12} \right] \tau_{sp}}{\left[\frac{I_p(\phi, \rho, z)}{h\nu_p} \sigma_{13} + \frac{I_L(\phi, \rho, z)}{h\nu_L} \sigma_{12} \right] \tau_{sp} + 1} N_T, \quad (\text{S5b})$$

Note that at for a 3-level system, at pump threshold, $I_p(\phi, \rho, z) \gg I_L(\phi, \rho, z)$, $N_2(\phi, \rho, z) - N_1(\phi, \rho, z) \ll N_T$, $\sigma_{12} \approx \sigma_{21}$. Therefore,

$$\begin{aligned} N_2(\phi, \rho, z) - N_1(\phi, \rho, z) &\approx \frac{\frac{I_p(\phi, \rho, z)}{h\nu_p} \sigma_{13} \tau_{sp} - 1}{\frac{I_p(\phi, \rho, z)}{h\nu_p} \sigma_{13} \tau_{sp} + 1} N_T = \left[1 - \frac{1}{\frac{1}{2} \left[\frac{I_p(\phi, \rho, z)}{h\nu_p} \sigma_{13} \tau_{sp} - 1 \right] + 1} \right] N_T \\ &\approx \left[1 - \left(1 - \frac{1}{2} \left[\frac{I_p(\phi, \rho, z)}{h\nu_p} \sigma_{13} \tau_{sp} - 1 \right] \right) \right] N_T = \frac{1}{2} \left[\frac{I_p(\phi, \rho, z)}{h\nu_p} \sigma_{13} \tau_{sp} - 1 \right] N_T. \end{aligned} \quad (\text{S6})$$

We obtain

$$\frac{dI_L(\phi, \rho, z)}{\rho d\phi} = \frac{1}{2} \left[\frac{I_p(\phi, \rho, z)}{h\nu_p} \sigma_{13} \tau_{sp} - 1 \right] N_T \sigma_{12} I_L(\phi, \rho, z) - \frac{2m_{iL}}{\rho} I_L(\phi, \rho, z). \quad (\text{S7})$$

At threshold, gain compensates loss, one may find the pump threshold according to

$$\bar{P}_{p,th} \approx \frac{h\nu_p}{\sigma_{13} \tau_{sp} N_T \sigma_{12}} \left(\frac{2m_{iL}}{R_0} + \frac{1}{2} N_T \sigma_{12} \right) \frac{\int dv \hat{I}_L(\rho, z)}{\int dv \hat{I}_p(\rho, z) \hat{I}_L(\rho, z)}. \quad (\text{S8})$$

One would find that according to the equation (Eq. **S8**) above, the minimum pump threshold occurs when the laser and pump mode intensity overlap $\Gamma = \int dv \hat{I}_p(\rho, z) \hat{I}_L(\rho, z)$ is maximized.